Equilibrium Temperature of an Unheated Icing Surface as a Function of Air Speed*

BERNARD L. MESSINGER†

Lockheed Aircraft Corporation

ABSTRACT

The thermal analysis of a heated surface in icing conditions has been extensively treated in the literature.[8] Except for the work of Tribus,[1] however, little has been done on the analysis of an unheated icing surface. This latter analysis is significant in the design of cyclic thermal deicing systems that are attractive for small high-speed aircraft for which thermal anti-icing requirements have become severe.

In this paper, a complete analysis of the temperature of an unheated surface in icing conditions is presented for the several significant régimes (i.e., less than 32°F., at 32°F., and above 32°F.) as a function of air speed, altitude, ambient temperature, and liquid water content.

The results are presented in graphical form and permit the rapid determination of surface temperature for a wide range of variables. Curves are presented to determine the speeds beyond which no ice accretion will occur. Curves are also presented to indicate the surface temperature and the rate of ice sublimation which takes place when an ice-covered surface emerges into clear air.

One significant result of this study is the introduction of a new basic variable referred to as the "freezing-fraction," which denotes the proportion of the impinging liquid which freezes in the impingement region. The fact that some of the liquid does not freeze in the impingement region tends to explain the observed variation in ice formation shape with temperature, speed, and water catch.

New test data obtained at Mt. Washington, N.H., for stagnation-point surface temperatures of an unheated plastic cylinder in natural and artificial icing conditions are included in the Appendix. These data substantiate the validity of the assumptions made in the theoretical analysis.

(1) INTRODUCTION

AIRFOILS MAY BE PROTECTED against icing in two basic ways. The ice may be entirely prevented from forming (anti-icing) as, for example, by thermal or chemical means; or it may be allowed to form to a tolerable thickness and periodically removed (deicing) as in the case of the inflatable boot or the cyclic application of heat. Until recently, almost all aircraft employed either an inflatable boot type of deicing or a thermal system of anti-icing, the latter being the preferred method.

Presented at the Design and Structures Session, Annual Summer Meeting, I.A.S., Los Angeles, June 27–28, 1951. Revised and received July 2, 1952.

* The author is indebted to M. M. Friedlander for assistance in preparation of the curves and to P. J. Valentine for suggestions relative to the "freezing fraction" concept. Both are members of the Thermodynamics Group at Lockheed Aircraft Corporation.

† Department Manager, Thermodynamics.

The advent of transonic aircraft speeds and very thin airfoils has made the application of thermal ice prevention extremely difficult or impractical, and, as a result, increased attention has been given to the possibilities offered by the cyclic thermal deicing method. The publication of reference 1 has been an important factor in directing attention to the significant economy of energy that is possible by the use of cyclic thermal deicing as compared to the continuous thermal anti-icing method. A more recent report, reference 2, contains experimental results of preliminary N.A.C.A. research with cyclic electrothermal deicing using a relatively low-intensity system. By using a short duration, high-intensity "on" period, the average energy can be of the order of one-tenth to one-twentieth of energy required for continuous anti-icing. This large reduction in energy requirements makes electrical power appear to be an ideal source of heat for a cyclic thermal system. These general characteristics have been experimentally verified by numerous flight and laboratory tests recently conducted by the Lockheed Aircraft Corporation.

Of the thermal types, the continuous anti-icing system has predominated in the last decade. Hence, the theoretical studies and methods of analysis developed in this period have been almost entirely concerned with the energy balance that exists when an anti-iced surface is maintained at a temperature considerably above the freezing point, generally at about 100°F. Little if any attention (except in reference 1) has been directed toward determining the temperature of an unheated icing surface.

If, in designing a cyclic thermal deicing system, high-intensity heating (about 30 to 40 watts per sq.in.) is used, a short "on" period as low as 2 sec. may be employed. This permits a ratio of "off" to "on" time of as much as 50 or 75 to 1. With this large a ratio of "off" time, the *initial temperature* of the iced surface just prior to an "on" period is essentially the *equilibrium temperature of an unheated airfoil surface.* Although the exact mechanics of the ice removal process in a cyclic thermal system is not fully understood, it is believed that this initial surface temperature has a significant bearing on the net energy required. Other factors that may be involved are related to the effect of ice thickness and liquid surface tension on the removal process. It was pointed out in reference 1 that one advantage of the deicing method is that a high rate of water catch results in a higher initial temperature in the ice impingement area due to the release of the latent heat of fusion, whereas an anti-icing system is severely taxed at high rates of water impingement because not only is the heat of fusion unavailable but, in addition, the entire latent heat of evaporation must be supplied, as well as the usual loss by convection heat transfer. By using high-intensity thermal deicing, it is possible to achieve nearly instantaneous, dry removal of ice, thus avoiding the effect of "runback" and consequent refreezing.

During the early phases of the development of aircraft ice-protection systems, it was usually assumed that, when the day came that airplanes would fly fast enough to result in stagnation temperatures of 32°F. or more, the problem of icing would be eliminated. As that day approached, however, it became increasingly obvious that the surface temperature rise in icing conditions would be different from that which would prevail in dry air. It is now evident that ice *can* be deposited on a surface even though the speed corresponds to a clear-air surface temperature of more than 32°F.

One of the early attempts to analyze the effect of free moisture on the kinetic heating of the boundary layer was made by J. K. Hardy, a visiting British anti-icing specialist who was temporarily stationed at the Ames Aeronautical Laboratory of the N.A.C.A. The results of his work were reported in 1944 in reference 3 and somewhat later in references 4 and 5. In reference 4, Hardy introduced the concept of a "datum temperature," which he considered to be a basic reference parameter for use in computing the unit heat- and mass-transfer rates for a heated surface in icing flight. This "datum temperature" parameter was adopted and used in many subsequent reports and articles on ice protection.[6–9] In some of these articles (particularly reference 6), the suggestion is made that the "datum temperature" cannot be measured in an icing cloud because of the release of the heat of fusion. In the opinion of the author of the present paper, there are certain fallacies in the manner in which the "datum temperature" parameter has been employed, and these will be discussed in detail later in the article.

It is the purpose of this paper to present a complete analysis of the conditions that govern the equilibrium temperature of an insulated, unheated surface exposed to icing. The analysis is, in part, based on the approach begun in reference 1 but goes beyond the scope of that work. The latter considered icing conditions for a surface temperature *above* and *below* 32°F. but not *at* 32°F. The present analysis includes an important range of conditions at a 32°F. surface temperature using the concept of the "freezing fraction." In extending the results of this analysis to the problem of airfoil ice protection, some consideration must be given to the limitations of some of the simplifying assumptions involved in certain of the parameters that are employed.

In that range of conditions in which a surface temperature of *more* than 32°F. is attained during icing, an analysis has also been developed using a parameter that will be referred to as the "evaporation fraction." This latter analysis includes conditions up to and including the speed for complete evaporation of all intercepted water.

Also of interest to the aircraft designer are those factors that govern the ability of the airplane to rid itself of ice accretions collected on unprotected surfaces after it has emerged from icing conditions into clear air. For this reason, an analysis is presented which permits the determination of (a) the rate of sublimation of ice from a surface at less than 32°F. in clear air, (b) the speed required to attain a surface temperature of 32°F. on an ice-covered surface in clear air, and (c) the rate of melting from a wet surface of ice at 32°F. in clear air.

(2) Symbols

A = surface area, sq.ft.
B = ambient absolute pressure, in. of mercury
b = "relative heat factor," $R_w c_w/f_c$, dimensionless
c_i = unit heat capacity of ice, B.t.u./lb. °F.
c_p = unit heat capacity of air, B.t.u./lb. °F.
c_w = unit heat capacity of water, B.t.u./lb. °F.
δ_m = linear melting rate, in. per hour
δ_s = linear sublimation rate, in. per hour
E_m = water droplet catch efficiency, dimensionless
f_c = unit convection conductance, B.t.u./hour ft.^{2} °F.
g = gravitational constant, 32.2 ft./sec.^{2} or lbs. per slug
γ_i = density of ice, lbs. per cu.ft.
J = mechanical equivalent of heat, 778 ft.lbs. per B.t.u.
L_e = latent heat of vaporization of H_2O, B.t.u. per lb.
L_f = latent heat of fusion of H_2O, B.t.u. per lb.
L_s = latent heat of sublimation of ice, B.t.u. per lb.
m = evaporation fraction, dimensionless
n = freezing fraction, dimensionless
P = vapor pressure of atmospheric moisture, in. of mercury
P_{si} = vapor pressure over ice at t_{s_e}, in. of mercury
P_{sw} = vapor pressure over water at t_{s_e}, in. of mercury
q = rate of heat flow, B.t.u. per hour [subscripts defined in paragraphs (3.1), (3.2), and (6.2)]
r = "recovery" factor applying to kinetic heating, dimensionless
R_w = unit rate of water catch, lbs./hour ft.^{2}
R_{we} = unit rate of evaporation of water, lbs./hour ft.^{2}
R_{wm} = unit rate of melting of water, lbs./hour ft.^{2}
t_∞ = ambient free-stream temperature, °F.
t_{s_e} = equilibrium surface temperature, °F.
θ = heat balance parameters, °F. [defined in paragraph (4)]
V_∞ = free-stream velocity, ft. per sec.

(3) Modes of Energy Transfer to an Unheated Icing Surface

(3.1) *Equilibrium Surface Temperature Less Than 32°F.*

For an icing surface having a steady-state temperature, t_{s_e}, of less than 32°F., the actual value of t_{s_e} will be largely dependent on the result of an energy balance involving the simultaneous interchange of the following quantities (see Fig. 1):

(3.1.1) Heat *lost* by convection:

$$q_c = f_c A(t_{se} - t_\infty)$$

(3.1.2) Heat *lost* by sublimation:

$$q_s = 2.90 L_s f_c A[(P_{si} - P_\infty)/B]^*$$

(3.1.3) Heat *lost* due to being absorbed by the warming of the impinging subcooled liquid:

$$q_w = R_w A c_w(32 - t_\infty)$$

(3.1.3) Heat *gained* due to the release of the latent heat of fusion as the subcooled liquid impinges and changes to the solid state at 32°F. and, then, as a solid, cools to t_{se}:

$$q_f = R_w A[144 + c_i(32 - t_{se})]$$

(3.1.5) Heat *gained* due to the viscous or frictional heating in the boundary layer:

$$q_v = f_c A(rV_\infty^2/2gJc_p)\dagger$$

(3.1.6) Heat *gained* equivalent to the kinetic energy of the liquid particles as they strike the icing surface:

$$q_k = R_w A(V_\infty^2/2gJ)$$

Because, in this case, the value of t_{se} is assumed to be less than 32°F., all of the impinging water is considered to have solidified so that no mass transfer by direct "blowoff" of liquid takes place and the accretion rate will be R_w. In addition, the effect of heat *loss* by radiation has been entirely disregarded, since it is relatively insignificant.

(3.2) t_{se} Equal to 32°F.

For a surface having an equilibrium temperature of 32°F., the energy balance is basically similar to that outlined above, *except* that an additional variable (hereafter referred to as the "freezing fraction," n) is involved in energy quantity (3.1.4). When operating conditions result in the value of t_{se} just reaching 32°F., n will be equal to 1.0, which signifies that *all* of the impinging liquid is converted to ice. When conditions correspond to the release of a somewhat greater net amount of heat to the ice formation (as with increased speed), part of the impinging water will not solidify but will persist as a 32°F. liquid, so that the value of n, the "freezing fraction," will be *less* than 1.0. Whenever n is less than 1.0, the heat quantity (3.1.2) corresponds to the latent heat of *evaporation* rather than heat of sublimation, even though a large part of the water may be present as ice.

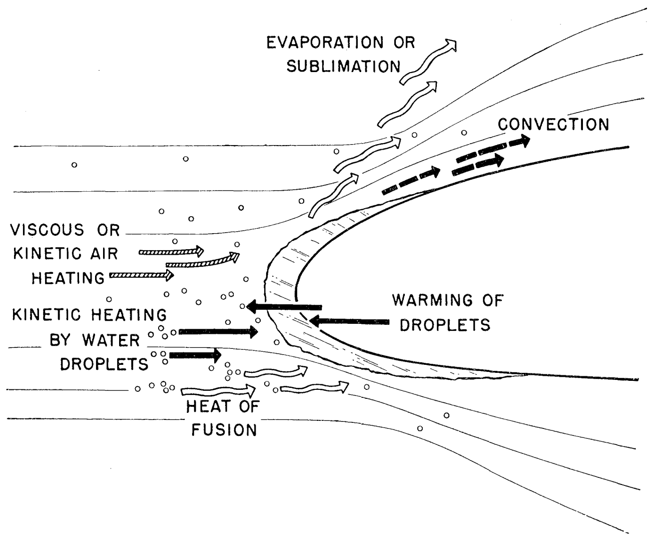

FIG. 1. Modes of energy transfer for an unheated airfoil in icing conditions.

The energy balance for a 32°F. surface temperature, t_{se}, in icing, therefore involves:

(3.2.1) Heat *lost* by convection:

$$q_c = f_c A(32 - t_\infty)$$

(3.2.2) Heat *lost* by evaporation (unless $n = 1$):

$$q_e = 2.90 L_e f_c A[(P_{sw} - P_\infty)/B]$$

(3.2.3) Heat *lost* due to warming of the liquid:

$$q_w = R_w A c_w(32 - t_\infty)$$

(3.2.4) Heat *gained* due to the latent heat of fusion:

$$q_f = 144 n R_w A$$

(3.2.5) Heat *gained* due to viscous or frictional heating:

$$q_v = f_c A(rV_\infty^2/2gJc_p)$$

(3.2.6) Heat *gained* due to the kinetic energy of the impinging liquid:

$$q_k = R_w A(V_\infty^2/2gJ)$$

As the value of n becomes smaller, it is probable that a significant part of the impinging liquid will leave the surface by "blowoff" or "runoff." When the value of n becomes zero, none of the impinging water freezes and the surface may be at 32°F. *or above.* Note that the actual ice accretion rate in this range will be equal to nR_w.

(3.3) t_{se} Greater Than 32°F.

For above-freezing surface temperatures, at least some of the impinging water will probably run off the trailing edge of the airfoil during actual icing conditions. At the same time, however, part of the impinging water

* The constant 2.90 is an empirical factor relating mass transfer to convection heat transfer. In reference 1 this constant appears erroneously as being equal to 2.29 because of a numerical error in the derivation. Also, to be completely accurate, the values of P_∞ and B should be replaced by their corresponding *local* values just outside the boundary layer. Thus the areas of low static pressure promote increased evaporation and high static pressure areas suppress evaporation. The magnitude of this effect is considered negligible in this paper.

† This term is usually combined with that of paragraph (3.1.1) to give the *net* convection loss.

will leave the airfoil by evaporation, and that fraction that is evaporated in the impingement area is denoted by the symbol, m, and can be determined analytically as will be shown in a later section. At certain conditions corresponding to $m = 1.0$, the net energy gained by the surface will permit *complete evaporation* of the impinging liquid; hence, there will be no runback and presumably the surface will approach a dry condition.

The energy balance for a surface temperature, t_{se}, greater than 32°F. in icing, therefore involves:

(3.3.1) Heat *lost* by convection:

$$q_c = f_c A(t_{se} - t_\infty)$$

(3.3.2) Heat *lost* by evaporation:

$$q_e = 2.90 L_e f_c A[(P_{sw} - P_\infty)/B] = mR_w L_e A$$

(3.3.3) Heat *lost* due to warming of the liquid:

$$q_w = R_w A c_w(t_{se} - t_\infty)$$

(3.3.4) Since *none* of the liquid freezes, there is no term representing the heat of fusion.

(3.3.5) Heat *gained* due to frictional heating:

$$q = f_c A(rV_\infty^2/2gJc_p)$$

(3.3.6) Heat *gained* due to the kinetic energy of the impinging liquid:

$$q_k = R_w A(V_\infty^2/2gJ)$$

(4) Evaluation of the Basic Heat Balance Equations

(4.1) When $t_{se} \leq 32°F$.

Arranging the terms of paragraph (3.1) in a single heat balance equation yields:

$$\text{Net heat loss} = q = f_c A\left[\left(t_{se} - t_\infty - \frac{rV_\infty^2}{2gJc_p}\right) + 2.90L_s\left(\frac{P_{si} - P_\infty}{B}\right)\right] +$$

$$R_w A\left[c_w(32 - t_\infty) - 144 - c_i(32 - t_{se}) - \frac{V_\infty^2}{2gJ}\right]$$

The last term can be evaluated at $c_w = 1.0$ and $c_i = 0.47$,

$$\ldots + R_w A[0.47t_{se} - t_\infty - 127 - (V_\infty^2/2gJ)]$$

By introducing* the dimensionless ratio $b = R_w c_w/f_c$ and three new groupings of the variables—namely,

$$\theta_1 = t_{se}(1 + 0.47b) + (2.90L_sP_s/B)$$

$$\theta_2 = t_\infty(1 + b) + (2.90L_sP_\infty/B) + 127b$$

$$\theta_3 = [(r/c_p) + b](V_\infty^2/2gJ)$$

the combined equation then becomes

$$q = f_c A(\theta_1 - \theta_2 - \theta_3)$$

For the case of an unheated surface under equilibrium conditions, $q = 0$ and therefore $\theta_1 = \theta_2 + \theta_3$.

For any given altitude, the function θ_1 can be plotted in terms of t_s and b; θ_2, in terms of t_∞ and b; and θ_3 for an arbitrary value of r [$r = 0.875$, a compromise value for laminar (0.85) and turbulent (0.90) flow],† in terms of V_∞ and b. Such plots are shown in Figs. 2, 3, and 4. These θ functions have the dimensions of temperature °F. and, except where they are independent of altitude, have been plotted for 20,000 ft.

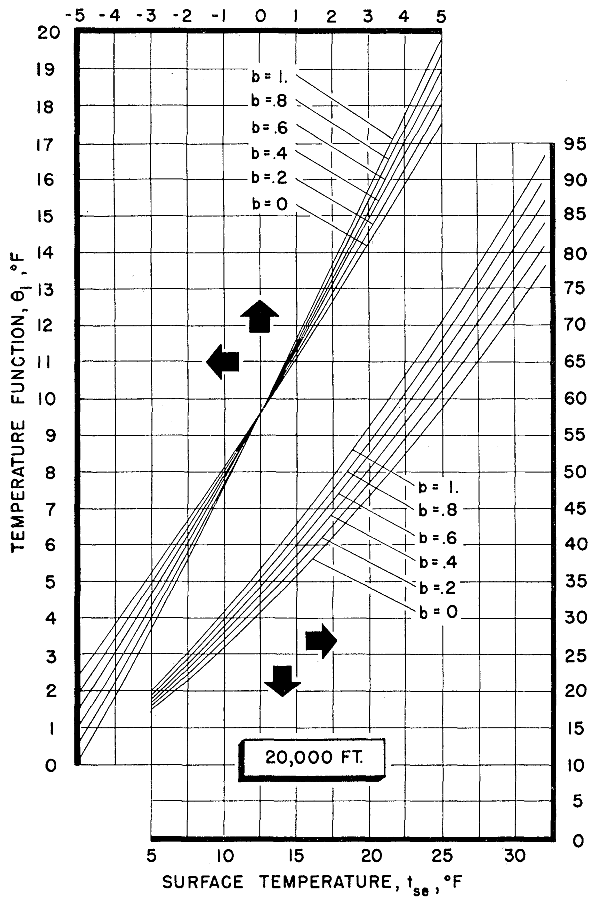

FIG. 2. Temperature function θ_1 versus surface temperature t_{se} for 20,000-ft. altitude.

* These parameters were first presented in reference 1.

† A more precise form for r is $[1 - (V^2/V_\infty^2)(1 - Pr^n)]$, where $n = 1/2$ for a laminar and $n = 1/3$ for a turbulent boundary layer.

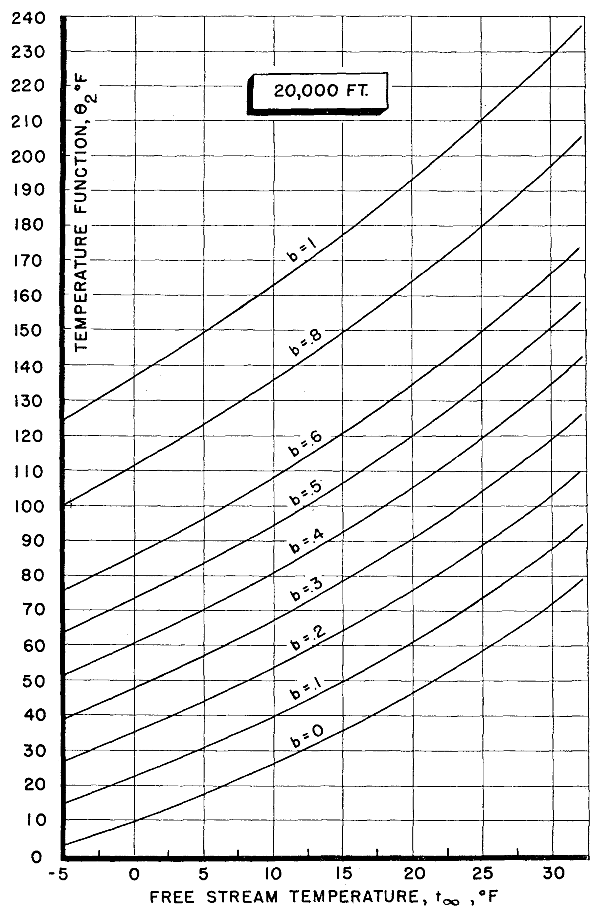

FIG. 3. θ_2 versus t_∞ for 20,000-ft. altitude.

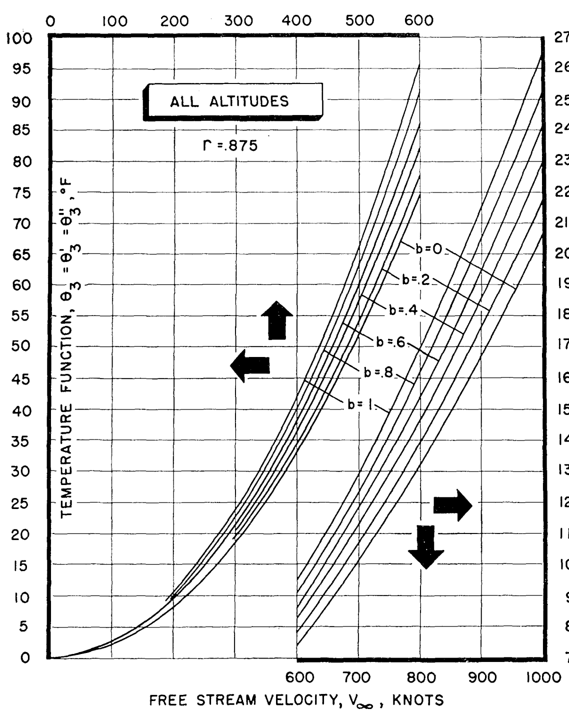

FIG. 4. θ_3, θ_3', and θ_3'' versus V_∞.

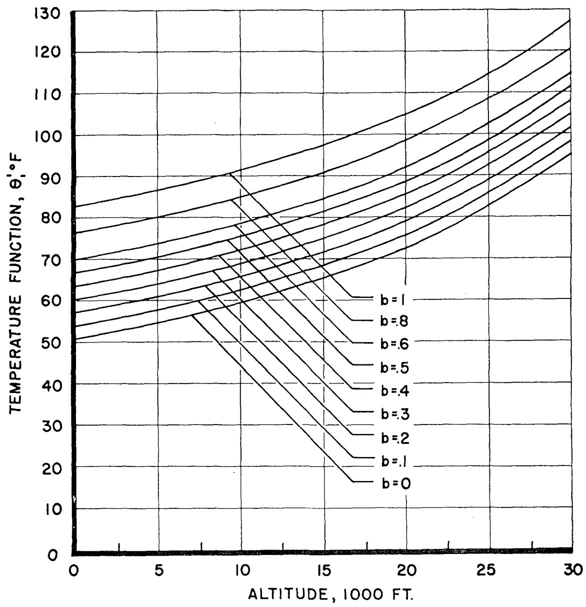

FIG. 5. θ_1' versus altitude.

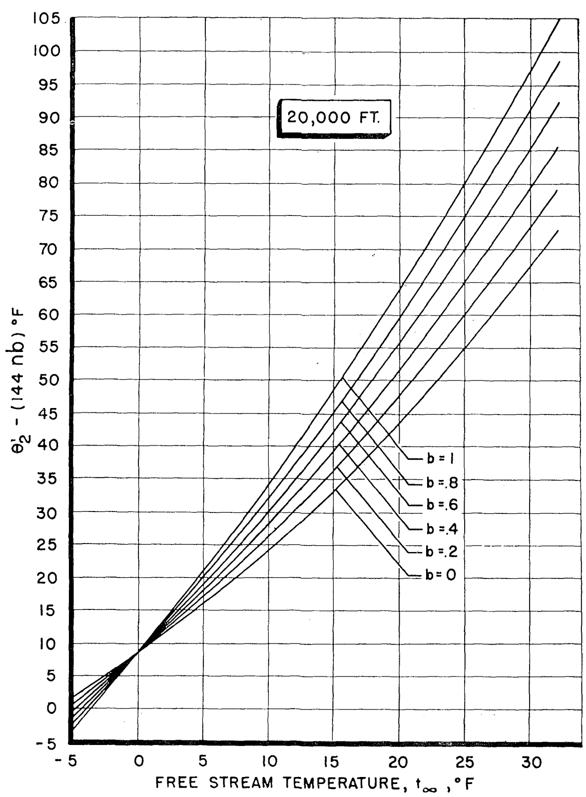

FIG. 6. θ_2' — $(144nb)$ versus t_∞ for 20,000-ft. altitude.

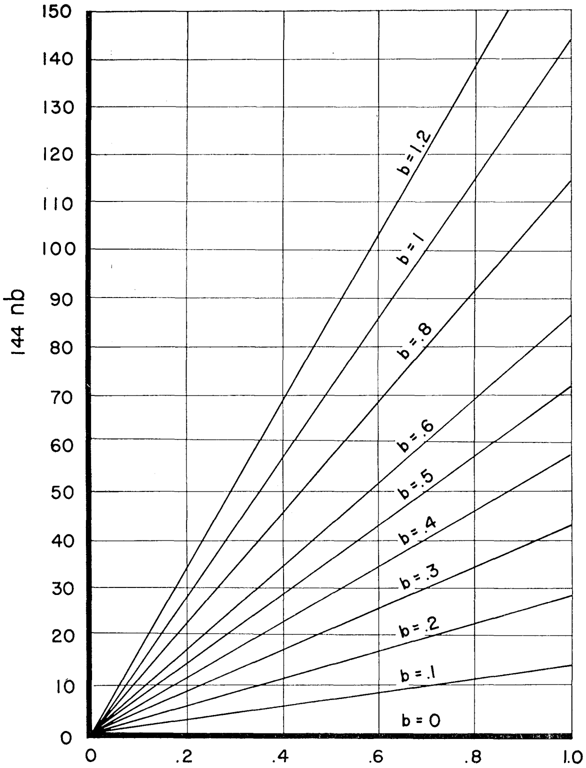

FIG. 7. Plot of $144nb$ versus n.

(*4.2*) ***When*** t_{se} $=$ ***32°F. and*** $0 < n < 1$

For this case, the terms of paragraph (3.2) can be conveniently correlated by means of a second group of θ' functions:

$$\theta_1' = 32(1 + b) + (560/B)$$

(based on $L_e = 1{,}075$ for $t_{se} = 32$°F.),

$$\theta_2' = t_\infty(1 + b) + (3{,}120P_\infty/B) + 144nb$$

$$\theta_3' = \theta_3 = [(r/c_p) + b](V_\infty{}^2/2gJ)$$

and also, in this case, since $q = 0$,

$$\theta_1' = \theta_2' + \theta_3'$$

For any given altitude θ_1' is a function only of b as shown in Fig. 5, and θ_2' can be plotted in two steps as indicated in Figs. 6 and 7.

(*4.3*) ***When*** $t_{se} \geq$ ***32°F. and*** $n = 0$

The terms of paragraph (3.3) can be expressed by a third group of θ'' functions:

$$\theta_1'' = t_{se}(1 + b) + (3{,}100P_s/B)$$

(based on $L_e \cong 1{,}070$ when 32°F. $< t_{se} <$ 50°F.),

$$\theta_2'' = t_\infty(1 + b) + (3{,}100P_\infty/B)$$

(based on $L_e \cong 1{,}070$ for 32°F. $< t_{se} <$ 50°F.), and

$$\theta_3'' = \theta_3' = \theta_3 = [(r/c_p) + b](V_\infty{}^2/2gJ)$$

and again

$$\theta_1'' = \theta_2'' + \theta_3''$$

As indicated in Fig. 8, both θ_1'' and θ_2'' can be represented by a single plot.

(*4.4*) ***When*** $t_{se} \geq$ ***32°F. and*** $n < 1$

In order to determine the extent of the evaporation in the impingement area when $t_{se} \geq$ 32°F. and $n < 1$, the following energy balance can be solved in terms of m, the evaporation fraction:

The energy required for evaporation:

$$q_e = mR_wL_eA$$

The energy available for evaporation:

$$q_e' = 2.9f_cL_eA[(P_{sw} - P_\infty)/B]$$

Equating the two forms,

$$m = \frac{2.9f_c}{R_w}\left(\frac{P_{sw} - P_\infty}{B}\right) = \frac{2.9f_c}{b}\left(\frac{P_{sw} - P_\infty}{B}\right)$$

This latter equation can also be used to determine the speed beyond which a surface exposed to icing conditions will be maintained *ice-free and dry* ($m = 1$):

$$P_{sw} = b(B/2.9) + P_\infty$$

After finding P_{sw}, the corresponding value of t_{se} can be found in any table of steam properties. The speed corresponding to this value of t_{se} can then be determined by means of Fig. 4 from $\theta_3'' = \theta_1'' - \theta_2''$.

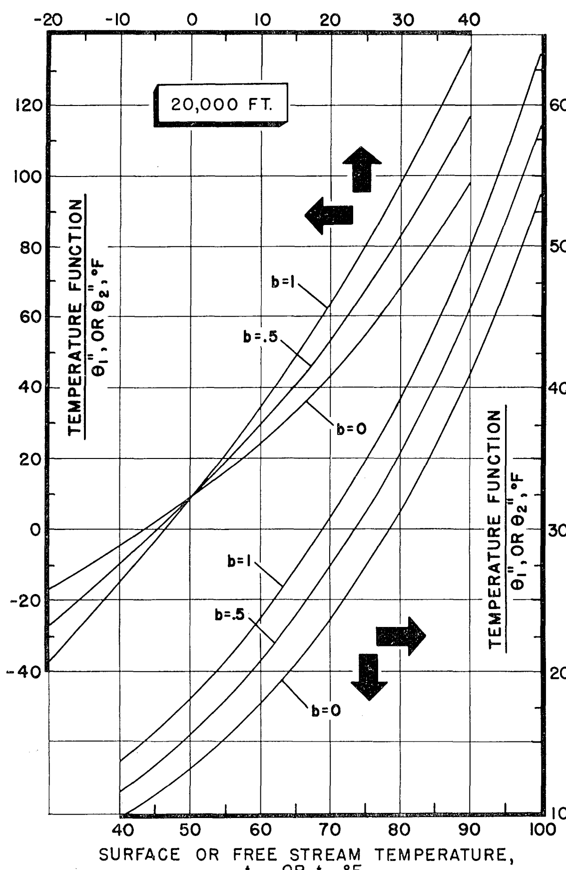

FIG. 8. θ_1'' versus t_{s_e} or θ_2'' versus t_∞ for 20,000-ft. altitude.

(5) Equilibrium Surface Temperature in Icing Conditions as a Function of the Significant Parameters

(5.1) Characteristics of the Parameters

By means of the graphical presentations of the θ functions, it is a simple matter to evaluate the heat balance equation and determine the equilibrium temperature t_{s_e} for any part of the range of flight speeds in icing conditions regardless of whether this temperature is above, at, or below the freezing point, provided, however, that the local value of b can be determined with reasonable accuracy.

The dimensionless ratio b (which is equal to $R_w c_w/f_c$) can be considered a measure of the ratio of the sensible heat-absorbing capacity of the impinging water per unit of surface area to the unit convective heat-dissipating capacity of the same surface. It has been proposed that this ratio be called the "relative heat factor."

No general statement can be made about the variations of the value of b except that, for a given position in the impingement area of an airfoil and for a constant air speed, it will vary directly as the liquid water content.

Another characteristic of the parameter, b, is that it tends to increase with altitude, since R_w increases and f_c becomes smaller for a given speed.

The variation of b with air speed depends, in turn, on the relationship between the variation of R_w and f_c with air speed for a given position on the airfoil. For an area in which the initial catch efficiency is close to 100 per cent, the value of R_w will vary directly with speed; if the initial catch efficiency is low, R_w will increase at a more rapid rate than the air speed. If the external boundary is locally laminar, f_c will vary as the square root of the air speed; if turbulent, it will vary as the 0.8 power of the air speed; in the transition region, it may vary as an air-speed power function greater than 1.0. It is therefore apparent that no simple single relationship will express the variation of b with air speed.

By making a survey of the local values of R_w and f_c around the periphery of a typical thin airfoil, it is possible to investigate the range of variation of b in the impingement area. Based on a laminar conductance, the maximum value of b is about three to four times the stagnation point value and seems to occur at about 5 per cent chord on the lower surface for an airfoil angle of attack at 4°. A typical stagnation point value for b is 0.5 based on a 6-ft. chord N.A.C.A. series 65-210 airfoil at 20,000 ft., 435 knots, 0°F., 30 micron drop size, and a liquid water content of 0.5 Gm. per cu.m.

A study of the θ function characteristics for equilibrium conditions yields the following relationships:

(5.1.1) θ_2 cannot be greater than θ_1 since θ_3 cannot be negative.

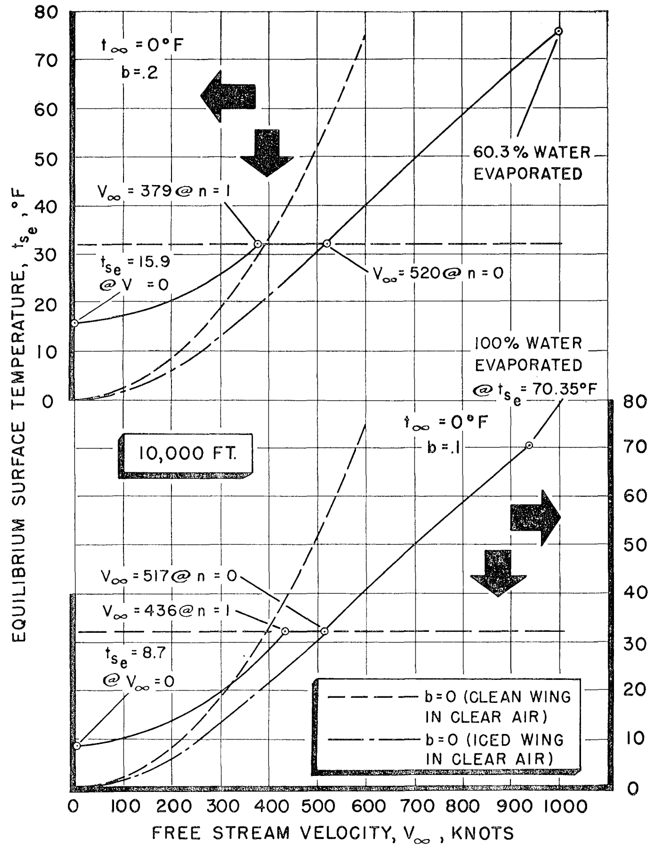

Fig. 9. t_{se} versus V for b_∞ = 0.1 and b = 0.2 at 10,000-ft. altitude.

(5.1.2) When $\theta_2 = \theta_1$, a purely hypothetical condition prevails—i.e., $\theta_3 = 0$ ($V_\infty = 0$)—and yet both water impingement and heat transfer are assumed to exist. This relationship, however, does establish the minimum t_{s_e} that can exist at subfreezing conditions for *a given value of b*. [See paragraph (5.2) and Fig. 10a for a detailed analysis of an actual condition.]

(5.1.3) If θ_2 is greater than that value of θ_1, which corresponds to 32°F., than n must be less than 1.0—i.e., *a wet icing surface exists*—and the θ' functions should be used.

(5.1.4) If $n = 0$ and $t_{s_e} = 32$°F., for a given value of t_∞, θ_2'' can be read directly and then subtracted from θ_1'' (corresponding to $t_{s_e} = 32$°F.) to give the required values of θ_3'' and thus the speed for *a surface that is wet but on which no ice is depositing*. This method was used to construct Fig. 11 from Fig. 4 and Fig. 8 for 20,000 ft. and from the equations for θ_1'' and θ_2'' of paragraph (4.3) for 10,000 and 30,000 ft.

(5.1.5) If the speed falls in the range between the two conditions defined by (5.1.3) and (5.1.4) above (i.e., $0 < n < 1$), the following steps can be used to determine the freezing fraction, n, for given values of V_∞, t_∞, b, and altitude or to determine V_∞ for given values of n, t_∞, b, and altitude:

(5.1.5.1) For the given value of altitude and b, determine the corresponding value of θ_1' using Fig. 5.

(5.1.5.2) If V_∞ is given, determine θ_3' using Fig. 4.

(5.1.5.3) Calculate $\theta_2' = \theta_1' - \theta_3'$.

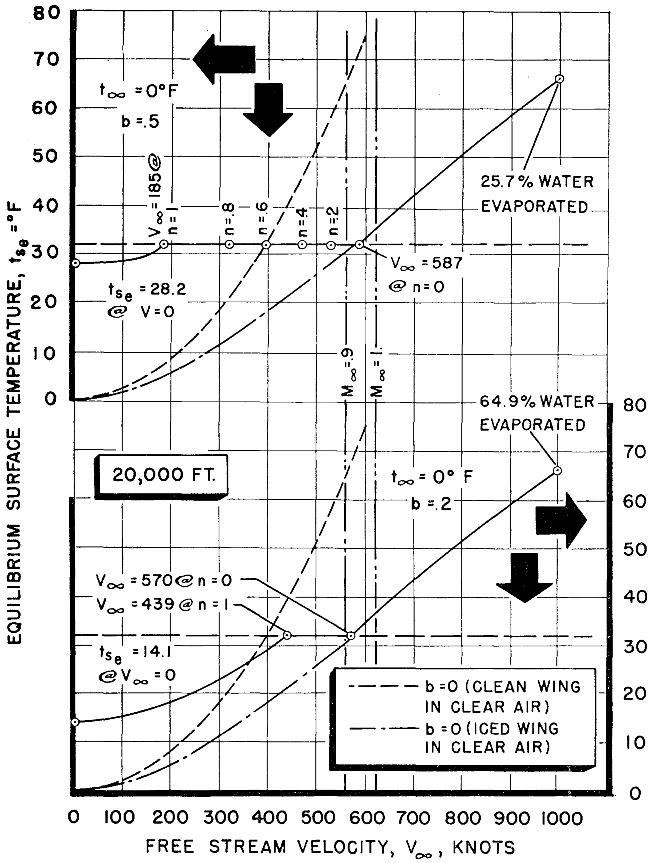

FIG. 10a. t_{se} versus V_∞ at b = 0.2 and b = 0.5 at 20,000-ft. altitude.

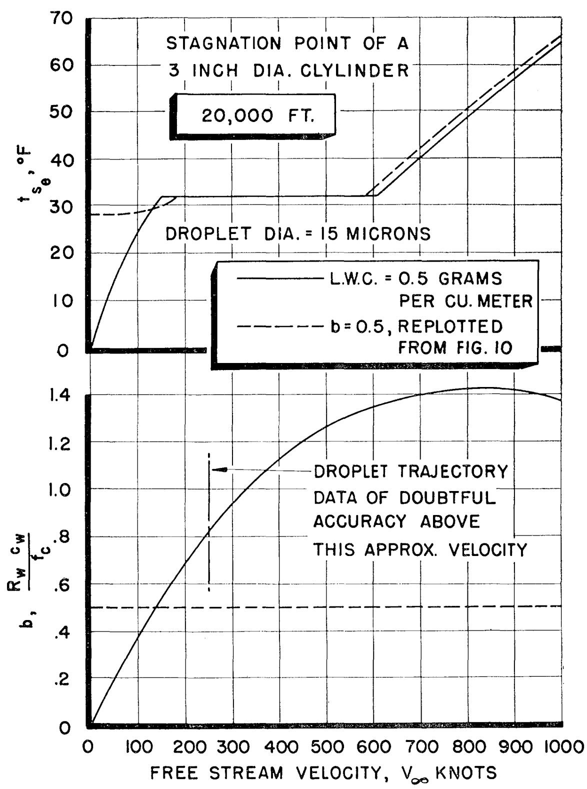

FIG. 10b. t_{se} versus V_∞ for variable value of b computed for constant liquid water content.

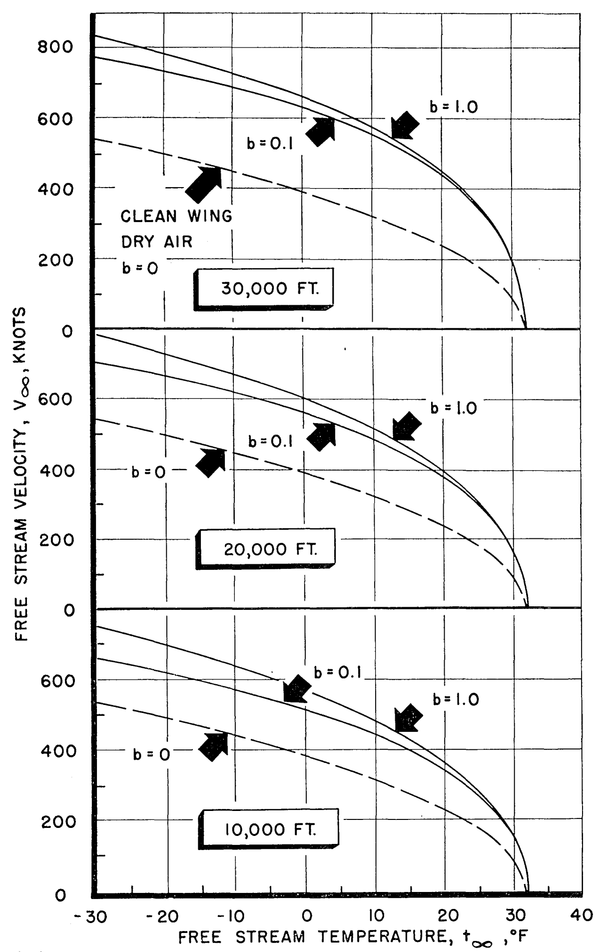

FIG. 11. V_∞ versus t_∞ for n = 0 at t_{se} = 32°F.

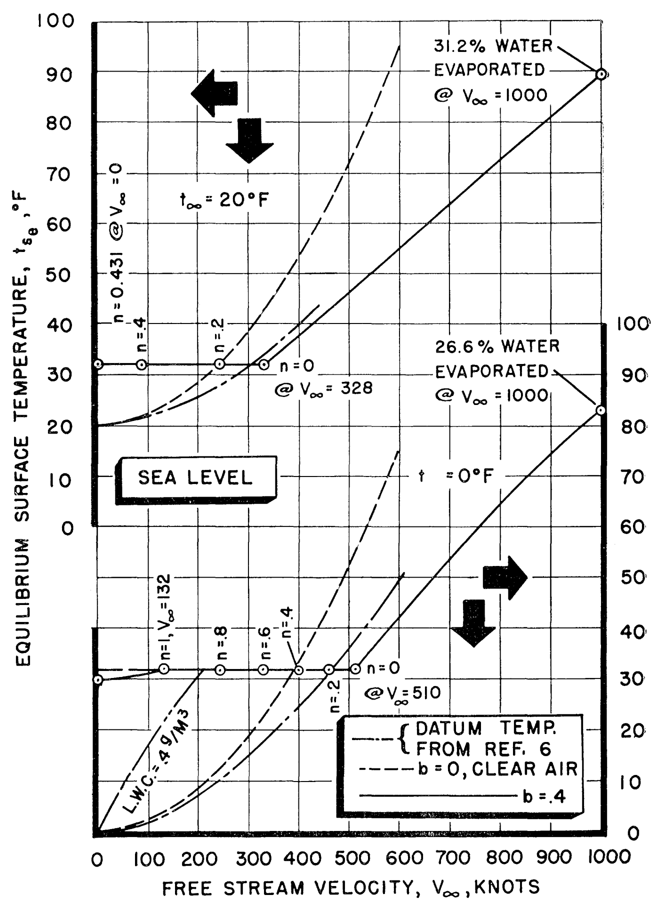

FIG. 12. t_{se} versus V_∞ at sea level for comparison with values replotted from reference 6.

(5.1.5.4) For given value of t_∞, determine $\theta_2' - (144nb)$ using Fig. 6, and then calculate $(144nb)$ using θ_2' as obtained in (5.1.5.3).

(5.1.5.5) Using Fig. 7, determine n for the given value of b.

(5.1.5.6) If n is a known value and it is necessary to determine the corresponding value of V_∞, then step (5.1.5.2) should consist of determining θ_2' by adding $(144nb)$ obtained from Fig. 7 to the value of $\theta_2' - (144nb)$ obtained from Fig. 6.

(5.1.5.7) Using Fig. 4, V_∞ can then be determined from θ_3', which is the sum of θ_1' and θ_2'.

(5.2) *Surface Temperature Characteristics*

In order to illustrate the general trend of t_{se} as a function of airplane altitude, speed, water catch rate, and surface conductance, Figs. 9 and 10 have been constructed by use of the θ functions of Parts (4.1), (4.2), and (4.3).

Although each of these plots of t_{se} versus air speed is shown for constant values of b, it should be noted that b will vary somewhat with speed as indicated above. It has been suggested by J. P. Lewis, one of the coauthors of references 2, 6, and 9, that, since Figs. 9, 10, and 12 do not present a realistic picture of the true variation of surface temperature with air speed, it would be desirable to construct these curves for constant values of liquid water content as would be the case in actual icing flight. Unfortunately, it is only possible to construct such a plot for a given location on a given configuration of aerodynamic body. In order to illustrate the differences between the general plot using b as the independent parameter and a specific plot using liquid water content as the independent parameter, Fig. 10a has been prepared based on the stagnation region of a 3-in. diameter cylinder. The lower part of the figure shows the variation of b with air speed for this point on the cylinder, and the shaded area of the upper part of the figure indicates the nature of the discrepancy that results from the use of the simplifying assumption that b remains constant. As noted on this figure, the accuracy of the catch efficiency in the higher speed range is doubtful, but it can be seen that a large variation in b has little influence on t_{se} at the higher speeds.

A line of constant liquid water content (= 0.4 Gm. per cu.m.) has also been added to the lower part of Fig. 12 to illustrate the same effect at sea level.

Fig. 10 shows that the effect of a high rate of water catch ($b = 0.5$) is to maintain the impingement area at 32°F. over a wide range of speeds, in this case from 185 to 587 knots. Note that, while a temperature of 32°F. is attained at only 185 knots, there is at least some ice accretion all the way up to 587 knots. Even at 395 knots for $b = 0.50$, Fig. 10 indicates that 60 per cent of the deposit is ice. There is as yet no experimental indication that, under these conditions, the liquid water present (40 per cent at 395 knots) acts in any way that would assist aerodynamic forces in blowing away the ice formation. In fact, a few high-speed icing flights have been unofficially reported for at least moderate icing conditions, at which time heavy, rapidly forming deposits of ice were observed. The liquid water present when $n < 1$ may form runback ice beyond the impingement region if the "wet adiabatic" surface temperature (see reference 6 curve in Fig. 12) is less than 32°F. for the air speed in question.

Plotted for comparison purposes in Figs. 9 and 10 are the dotted curves of t_{se} for (a) an ice-free surface in clear air and (b) an ice-covered surface in clear air.

In the lower part of Fig. 10 is a plot of the same variables at the same altitude but for a lower water-catch rate ($b = 0.2$). Note that the speed at which $n = 0$ (ice-free) is almost as high (570 knots) as the corresponding speed for $b = 0.5$ (587 knots).

Note by comparing Figs. 9 and 10 that, for a given value of b (in this case 0.2), the effect of changing altitude from 10,000 to 20,000 ft. (without changing the ambient temperature) is to lower t_{se} slightly at all speeds (except in the 32°F. range), which fact is undoubtedly due to the increased rate of evaporation or sublimation due in turn to the lower barometric pressure.

Certain general conclusions can be drawn from a study of the four comparative plots. These are:

(a) *High rates of water catch* (and correspondingly high values of b) tend to produce higher surface temperatures in the range of speeds up to about 500 knots.

(b) In the speed range up to that for $n = 1$ (dry surface of ice) for a given value of ambient temperature, speed, and b, the surface temperature decreases slightly with altitude.

(c) The speed beyond which the surface is ice-free, even in moderate icing conditions, is much higher than the speed for a 32°F. clean surface temperature in clear air. For example, in Fig. 10 the speed for $n = 0$ and $b = 0.5$ is 587 knots compared with 393 knots for a 32°F. surface at $b = 0$.

Fig. 11 was plotted to show how this critical ice-free speed at $n = 0$ and $t_{se} = 32$°F. varies with b, t_∞, and altitude.

(5.3) *"Wet Adiabatic" or "Datum Temperature"*

As indicated in Part (1), the "datum temperature" developed in reference 4 and later used in references 6, 7, 8, and 9 has been employed in the past as a measure of the temperature of an unheated icing surface. The following form of this parameter has been copied from reference 8:

$$t_{0_k} = t_0 + \frac{V^2}{2gJc_p}\left[1 - \frac{U^2}{V^2}(1 - Pr^{1/2})\right] - 0.622\,\frac{L_s}{c_p}\left(\frac{e_{0_k} - e_1}{P_1}\right)$$

where

t_{0_k} = datum temperature
t_0 = ambient static temperature
V = free-stream velocity
U = local velocity just outside the boundary layer
Pr = Prandtl Number
L_s = latent heat of vaporization (L_e)
e_{0_k} = saturation vapor pressure of water at t_{0_k}
e_1 = saturation vapor pressure of water just outside of the boundary layer
P_1 = barometric pressure just outside the boundary layer

The term within the bracket represents the local recovery factor.

An examination of the above equation indicates that this parameter might be more aptly named the "dynamic wet bulb temperature" rather than "datum temperature." Since it does not include terms to account for the sensible heating of the impinging droplets or the release of the latent heat of fusion, it cannot represent the true equilibrium temperature of an unheated icing surface or even the temperature of a surface that is wetted by an above-freezing-temperature cloud. It does represent the temperature in clear air of a surface that is wetted by water (possibly from within the surface) supplied at the temperature of the surface itself. This corresponds exactly to the wet bulb temperature and, as defined by the above equation, is in a general form that can be evaluated at any velocity. In fact, it is this form that permits the determination of the ambient wet bulb temperature from data obtained in high-speed flight.

Of related interest is the fact that in references 6, 8, and 9 the basic equation for the energy transfer from a heated airfoil contains two terms that are based on this "dynamic wet bulb" temperature. The convection loss term is presented as

$$q_c = f_c(t_s - t_{0_k})$$

which would indicate that the difference between surface temperature and wet bulb temperature is the controlling potential. This is obviously contrary to the definition of the conductance. If this were actually the case, there could be no wet bulb thermometer depression at low velocity, since the convection gain that just balances the evaporation loss would be zero because the wick surface would itself be at the wet bulb temperature and, hence, the above definition would not permit the transfer of heat by convection to the wick.

Similarly, the evaporation term is stated in these references as

$$q_e = f_c(X - 1)(t_s - t_{0_k})$$

or

$$q_e = f_c \frac{0.622L_s}{c_p}\left(\frac{e_s - e_{0_k}}{P_1}\right)$$

Here again, there could be no mass transfer from the wet bulb thermometer, since in this case e_s would be equal to e_{0_k} and the evaporation term would be zero.

Fortunately, the two terms q_c and q_e are invariably used in combination with each other in solving anti-icing design problems, and, because of the definition of the term X,

$$X = 1 + \frac{0.622L_s}{c_pP_1}\left(\frac{e_s - e_{0_k}}{t_s - t_{0_k}}\right)$$

the sum of the above two terms is equivalent to the sum of the two corresponding conventional terms:

$$q_c + q_e = f_c\left(t_s - t_0 + r\frac{V^2}{2gJc_p}\right) + f_c\left(\frac{0.622\,L_s}{c_p}\right)\left(\frac{e_s - e_1}{P_1}\right)$$

which satisfy the requirements of the psychrometric energy balance. The use individually of either of the terms of q_c or q_e as defined in references 6, 7, 8, and 9 would yield inaccurate results.

In order to illustrate the nature of the divergence between the results obtained by the methods of the present paper and those of references 6, 7, 8, and 9, Fig. 12 has been prepared. Curves of "datum temperature" for two ambient temperatures, 0° and 20°F., were copied directly from Fig. 2 of reference 6. The curves of t_{se} are plotted for an arbitrary value of b. Note that the region of greatest divergence is in the speed range below 300 to 400 knots, where the effect of the latent heat of fusion is noticeable. In the higher speed range, the difference between the two curves is small and is apparently due entirely to the cooling effect of the impinging liquid which is not taken into account in the datum temperature.

(6) Modes of Energy Transfer to an Unheated Ice-Covered Surface in Clear Air

(6.1) t_{s_e} Less Than, or Just Equal to, 32°F.

(6.1.1) Heat *lost* by convection:

$$q_c = f_cA(t_{se} - t_\infty)$$

(6.1.2) Heat *lost* by sublimation:

$$q_s = 2.90L_sf_cA[(P_{si} - P_\infty)/B]$$

(6.1.3) Heat *gained* due to viscous heating:

$$q_v = f_cA(rV_\infty{}^2/2gJc_p)$$

(6.2) t_{e_s} Greater Than 32°F. (Wet Ice Surface)

When the air speed of the ice-covered surface is sufficient to result in the surface temperature t_{se} exceeding the melting point, a rather complex condition exists.

A water film of some indeterminate thickness will cover the surface of the ice. The thickness of this film will be related to factors such as the liquid-surface tension and viscosity, as well as the boundary-layer drag forces. The net heat gained due to the viscous heating can only produce melting in the ice after having traversed the liquid film by conduction. A film of finite thickness will therefore contain a finite temperature gradient, the differential being (t_{se} − 32°F.) since the melting ice temperature can only be 32°F.

The water that is evolved in the melting process may leave the surface by two means: (a) evaporation or (b) mechanical blowoff or runoff. It has been determined by the numerical evaluation of typical operating conditions that the ice will be melted much more rapidly than it can be evaporated, and therefore most of it will leave the airfoil by mechanical runoff. For example, in order for the rate of evaporation to equal the rate of melting at a speed of 800 knots at an altitude of 10,000 ft. and a conductance of 20 B.t.u./hour °F. ft.^{2}, the equilibrium thickness of the water film would have to be 0.45 in., an unlikely condition. If it were possible for a water film of this thickness to persist, it would involve a temperature differential of 31°F. between the ice face and the external surface of the water film. If, as is probably the case, the actual film thickness is small—say, for example, 0.001 in.—its thermal resistance is small, and it has been determined that little error is involved if it is entirely neglected as was the case in constructing the curves of Fig. 15.

The energy balance, based on this latter assumption for a wet melting ice surface just slightly above 32°F. will therefore include the following terms:

(6.2.1) Heat *lost* by convection:

$$q_c = f_cA(t_{se} - t_\infty) \cong f_cA(32 - t_\infty)$$

(6.2.2) Heat *lost* by evaporation:

$$q_e = 2.90f_cL_eA[(P_{sw} - P_\infty)/B] \cong 2.90f_cL_eA[(0.1803 - P_\infty)/B]$$

(6.2.3) Heat *lost* by melting of ice:

$$q_m = R_{wm}AL_f$$

(6.2.4) Heat *gained* by viscous heating:

$$q_v = f_cA(rV_\infty^2/2gJc_p)$$

(7) Sublimation and Melting Rates from an Unheated Ice-Covered Surface in Clear Air

(7.1) *Sublimation*

The combined heat balance equation for the terms listed in Part (6.1) can be written as

$$q_v - q_c = q_s$$

or

$$f_cA\left[t_\infty + \left(\frac{rV^2}{2gJc_p}\right) - t_{se}\right] = 2.9L_sf_cA\left(\frac{P_{si} - P_\infty}{B}\right)$$

In the latter form, this equation can be evaluated for arbitrary values of t_∞, P_∞, and B in terms of V_∞ and t_{se}. In order to avoid a trial-and-error solution, t_{se} is selected as the independent variable.

Having obtained t_{se} in terms of V_∞, it is then possible to determine the rate of sublimation R_{ws} or $\gamma_i\delta_s/12$ from

$$q_s = 2.9L_sf_cA[(P_{si} - P_\infty)/B] = \gamma_i(\delta_s/12)L_sA$$

Since P_{si} has already been determined, it is possible to determine $\gamma_i\delta_s$ for an arbitrary series of values of f_c.

Fig. 13 is a plot of such values for three altitudes. The corresponding ambient temperatures for each altitude are N.A.C.A. standard.

The right-hand terminal points of each series of curves in Fig. 13 occur at the speed for a 32°F. surface temperature, and a general plot corresponding to these points is given in Fig. 14.

Note that in Fig. 13 the rate of sublimation is generally small, so that, once ice has accumulated on an airplane, its removal by sublimation alone is a slow process. Note also that for a given value of f_c the rate of sublimation at 32°F. (right end of each curve) is greater at high altitude than at low altitude, principally because of the lower value of B and also of P_∞. For a given speed the removal rate at high altitude is slower due entirely to the lower ambient temperature assumed. It is significant that these high-altitude removal rates would probably require more time for shedding even a minor ice accretion than the entire duration of an in-

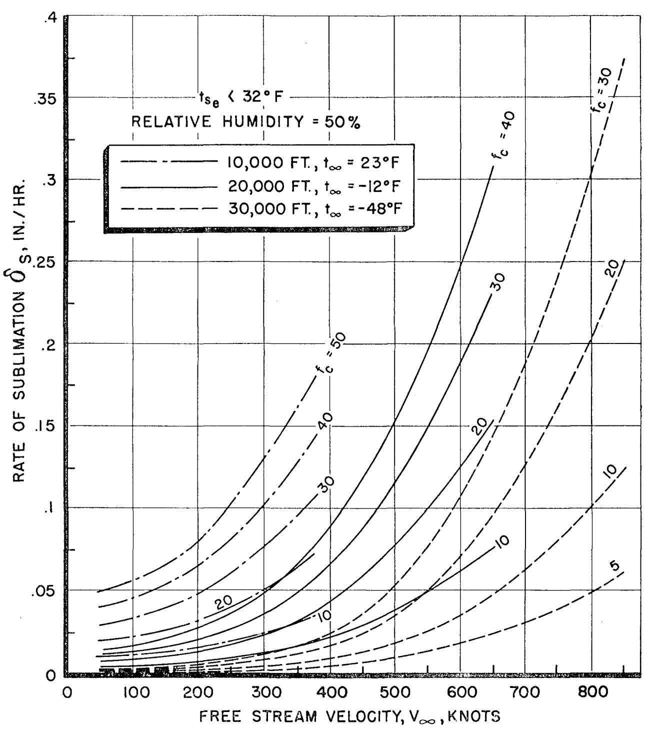

FIG. 13. Rate of sublimation of ice, δ_s versus V_∞ in clear air.

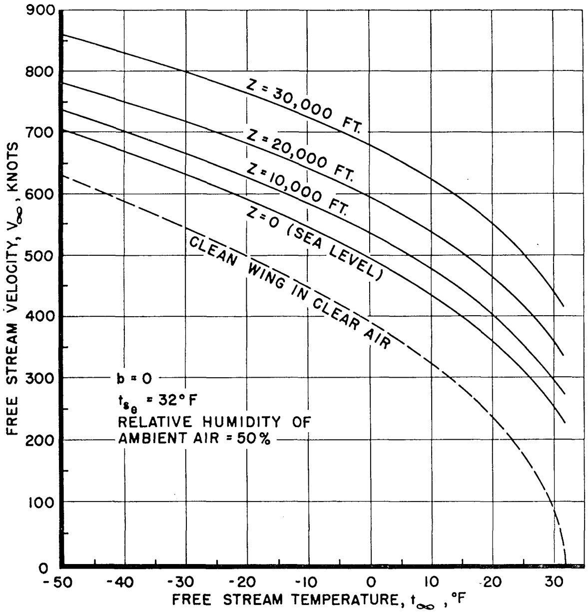

FIG. 14. V_∞ versus t_∞ for ice surface at 32°F. in clear air.

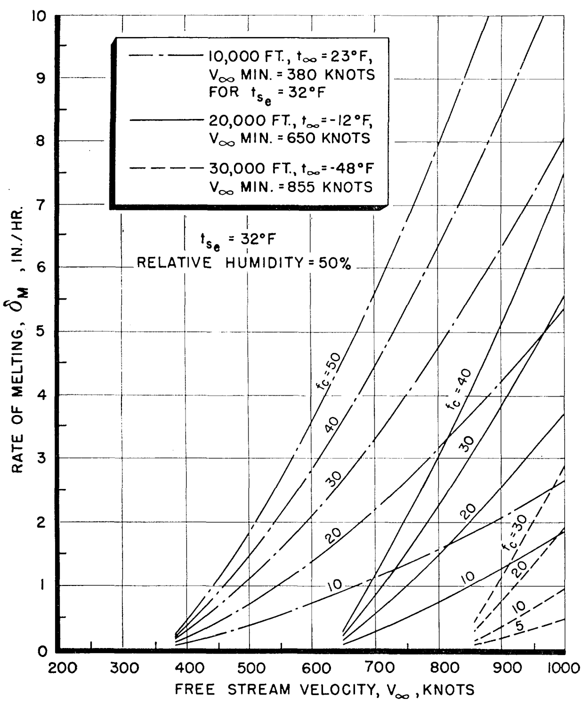

FIG. 15. Rate of melting of ice, δ_m versus V_∞ in clear air.

terceptor type of aircraft, the high-speed performance of which might be seriously crippled.

(7.2) Melting

When the speed exceeds the values given by Fig. 14, a wet surface will exist and the controlling factor for ice removal is the melting rate, although as indicated in Part (6.2) evaporation also occurs but its contribution to the removal is small compared to the runoff rate resulting from the melting.

The combined heat balance for the terms of paragraph (6.2) is

$$q_v - q_c - q_e = q_m$$

or, since $t_{se} = 32$°F.,

$$f_cA\left[t_\infty - \left(\frac{rV_\infty^2}{2gJc_p}\right) - 32\right] - 2.9L_ef_cA\left(\frac{0.1803 - P_\infty}{B}\right) = \gamma_i(\delta_m/12)L_fA$$

This equation was evaluated for the same arbitrary series of conditions used in Part (7.1), and the results are plotted in Fig. 15. Note that, although the melting rates are high, the speeds required to achieve them are also high.

In using Fig. 13 or 15 it should be remembered that, as the speed increases, the value of f_c also increases, so that for a given airfoil the sublimation or melting rate will increase faster with speed than indicated by the slope of the lines of constant f_c.

(8) Conclusions

At least some ice can collect on an unheated surface in normal low-temperature icing conditions at speeds up to about 600 knots (690 m.p.h.).

High rates of water catch tend to maintain an unheated icing surface at 32°F. over a wide range of speeds, but, except at the high speed end, a 32°F. surface temperature does not signify an ice-free surface.

Surface temperatures predicted by the "datum temperature" or "wet adiabatic" method of analysis are lower in the low-speed range and slightly higher in the high-speed range than are obtained by the methods developed in this paper.

Once an unheated surface has been allowed to collect ice, the period required to remove it by sublimation alone is long. It is of the order of 5 hours for $^1/_4$ in. of ice at an air speed of 500 knots at 30,000 ft. and N.A.C.A. standard ambient temperature.

The air speed required to attain a 32°F. ice surface temperature in clear air at 30,000 ft. and at N.A.C.A. standard temperature is about 850 knots. Beyond this speed, melting and evaporation occur.

There are few reliable experimental data available which would permit checking the accuracy of the results developed analytically in this paper. Such data, obtained in natural icing conditions, would be valuable for establishing the validity of the various foregoing assumptions (see Appendix).

References

[1] Tribus, Myron, *Intermittent Heating for Protection in Aircraft Icing*, University of California, Los Angeles, Ph.D. Thesis, August, 1949. (See also A.S.M.E. Trans., Vol. 73, No. 8, p. 1117, November, 1951.

[2] Lewis, James P., and Bowden, Dean T., *Preliminary Investigation of Cyclic De-icing of an Airfoil Using an External Electric Heater*, N.A.C.A. Research Memorandum No. R.M. E51J30, February 4, 1952.

[3] Hardy, J. K., *An Analysis of the Dissipation of Heat in Conditions of Icing from a Section of the Wing of the C-46 Airplane*, N.A.C.A. T.R. No. 831, 1945.

TABLE 1

EQUILIBRIUM STAGNATION POINT TEMPERATURE OF AN UNHEATED LUCITE CYLINDER IN MT. WASHINGTON ICING TUNNEL

January 7 to 21, 1952 — Cylinder Diameter = 3.75 inches

Run Number	Type of Icing:- N=Natural; A=Artificial	True Airspeed M.P.H	Liquid Water Content Grams/Cubic Meter	Droplet Diameter Microns	°F Wet Static Temperature (Equivalent Ambient)	°F Tunnel Total Temperature (Actual Ambient)	Droplet Reynolds Number R_u	Scale Modulus	Stagnation Point Water Catch Ratio	b, Relative Heat Factor	θ_3 or θ_3' *	θ_2 or θ_2' *	θ_1 or θ_1' *	n, Calculated Freezing Fraction	°F Calculated Surface Temperature	°F Measured Surface Temperature
1	A	244	.64	6.8	6.8	14.5	43.1	122.8	.18	.275	10	52.3	62.3	1.0	31.1	31.
2-A	A	252	.70	9.7	4.6	13.2	63.8	86.	.31	.527	11.3'	62.7'	74.0'	.65	32.	34.
2-B	A	252	2.00	7.6	4.6	13.2	49.9	110.	.22	1.065	12.5'	78.7'	91.2'	.402	32.	31.
2-C	A	252	.26	10.5	4.6	13.2	69.1	79.5	.335	.211	10.5	40.1	50.6	1.0	26.3	27.
3	A	235	1.10	8.5	10.1	16.8	51.6	98.2	.25	.645	10.1'	67.9'	78.'	.46	32.	33.
4	A	226	.32	12.0	0.9	8.3	71.3	69.5	.375	.276	8.5	41.95	50.45	1.0	25.8	25.
5	A	227	.27	20.7	4.1	11.	122.8	40.35	.59	.367	9.0'	59.6'	68.6'	.90	32.	30.
6-A	N	221	.27	9.8	5.4	11.7	56.5	85.2	.29	.178	7.9	36.6	44.5	1.0	23.4	22.
6-B	N	207	.27	10.	6.2	11.5	53.8	83.5	.29	.17	6.9	37.2	44.1	1.0	23.3	21.
7	A	220	.50	18.2	6.7	13.3	103.9	45.9	.53	.603	8.6'	64.6'	73.2'	.535	32.	32.
8	A	210	.81	17.1	17.9	22.7	91.2	48.8	.50	.90	8.5'	77.5'	86.'	.237	32.	33.
9	N	238	.70	16.4	12.8	19.0	94.5	50.9	.495	.796	9.4'	73.1'	82.5'	.35	32.	33.
10	N	234	.16	13.8	2.5	10.0	84.6	60.5	.44	.165	8.9	30.4	39.3	1.0	20.4	20.
11	N	228	.43	13.2	20.8	26.5	75.8	63.3	.41	.407	9.1'	60.9'	70.0'	.282	32.	31.
12-A	N	243	.17	8.9	0.8	9.0	56.9	93.8	.27	.107	9.4	20.9	30.3	1.0	16.	16.
12-B	N	243	.145	10.0	-0.2	7.7	64.0	83.5	.32	.111	9.4	19.1	28.5	1.0	15.2	18.
13	A	238	.34	13.0	7.7	14.7	80.1	64.2	.415	.334	9.7'	58.1'	67.8'	.83	32.	31.
14	N	232	.34	16.0	15.7	22.0	94.5	52.1	.49	.388	9.4'	59.8'	69.2'	.475	32.	32.

* The θ values shown are based on an average tunnel static altitude of 7800 feet. It was subsequently found that the actual average tunnel altitude was more nearly 8200 ft. but the θ values have not been revised since the net effect on t_{s_e} is believed to be small.

[4] Hardy, J. K., *Kinetic Temperature of Wet Surfaces, A Method of Calculating the Amount of Alcohol Required to Prevent Ice, and the Derivation of the Psychrometric Equation*, N.A.C.A. A.R.R. No. 5G13, September, 1945.

[5] Hardy, J. K., *Protection of Aircraft Against Ice*, Royal Aircraft Establishment, Report No. S.M.E. 3380, July, 1946.

[6] Gelder, Thomas F., and Lewis, James P., *Ice Protection for Turbojet Transport Airplane, Part II—Determination of Heat Requirements*, Institute of Aeronautical Sciences, Sherman M. Fairchild Fund Paper No. FF-1, March 24, 1950.

[7] Lewis, William, *Meteorological Factors in the Design and Operation of Thermal Ice Protection Equipment for High Speed, High Altitude Transport Airplanes*, Part 7 of a Compilation of the Paper Presented at N.A.C.A., "Conference on Some Problems of Aircraft Operation," October 9 and 10, 1950.

[8] Neel, Carr B., Jr., Bergrun, Norman R., Jukoff, David, and Schlaff, Bernard A., *The Calculation of the Heat Required for Wing Thermal Ice Prevention in Specified Icing Conditions*, N.A.C.A. T.N. No. 1472, December, 1947.

[9] Gelder, Thomas F., and Lewis, James P., *Comparison of Heat Transfer from Airfoil in Natural and Simulated Icing Conditions*, N.A.C.A. T.N. No. 2480, September, 1951.

APPENDIX

Since the time of the original presentation of this paper, the Lockheed Aircraft Corporation conducted a series of icing tests at the Aeronautical Ice Research Laboratory, Mt. Washington, N.H., which facility is operated jointly by the U.S. Air Force and the Navy Bureau of Aeronautics. One phase of this test program included a series of surface temperature measurements on an unheated Lucite cylinder, which had a 3.75-in. outside diameter and a 1/8-in. wall thickness and was approximately 12 in. long. Surface thermocouple readings were obtained at the forward stagnation point, as well as at the 100° and 180° positions.

The principal purpose of recording these cylinder temperatures was to obtain experimental data with which to check the validity of the theoretical analysis presented in the subject paper.

The test facility used for this investigation consisted of a duct attached to the inlet of a radial-flow jet engine. This duct, having a cross-sectional area of approximately 3 sq.ft., acted as a small icing wind tunnel by induction of the ambient icing cloud conditions that prevail at the top of Mt. Washington during the winter months of the year. By this means, the natural icing conditions which flow over the mountain top at velocities ranging from about 30 to 90 m.p.h. are accelerated in this tunnel to about 250 m.p.h.

Table 1 contains the data obtained for 18 individual icing runs under a variety of meteorological conditions. Rotating multiple cylinders were used to obtain the liquid water content and mean droplet diameter in the vicinity of the test cylinder. The ambient temperature of the air prior to its entry into the tunnel was taken to be the most reliable measure of the actual tunnel total temperature. The equivalent flight ambient temperature was then computed from this total temperature by making an allowance for the adiabatic acceleration of the water-laden air, including the effect of condensation of additional moisture due to the cooling of the air-water mixture resulting from the acceleration.

From the mean droplet diameter data shown, the corresponding droplet Reynolds Number R_u and Scale modulus ψ were computed. These values permitted the determination of the stagnation point water catch ratio (or catch efficiency) β_0 and, finally, the theoretical value of b, the relative heat factor. The θ values shown in the table were determined by using the θ curves of the subject paper, together with a set of unpublished curves which permitted correcting the θ values to the altitude indicated in the note under the table.

From the θ values, the theoretical value of n, the freezing fraction, and t_{se}, the equilibrium stagnation point temperature, were determined. In the last column the actual measured values are tabulated for comparison. The agreement is extremely good in spite of the obvious limitations of the instrumentation. For example, in Run No. 2A, a measured temperature of 34°F. is indicated even though the cylinder is unheated, an ice formation was observed in the thermocouple region, and the *total* temperature of the tunnel was 13.2° F. Similarly, the measured temperatures of 33°F. in runs 3, 8, and 9 indicate that the thermocouple inaccuracy was as high as 1 or 2°F. under some conditions. It is interesting to note that, in runs 5 and 13 where the predicted values of t_{se} are 1° or 2° higher than the measured, the value of n is only slightly less than 1.0, which would be the true value of n based on the *measured* temperature.

Note in the second column that the proportion of the runs obtained in natural icing was about equal to that using artificial spray water icing. The fact that the agreement in the last two columns did not appear to be influenced by this factor is an indication that, under the proper control, artificial icing is a valid research technique. The fact that it has been reported to the writer that the full effect of the latent heat of fusion has not been observed in the N.A.C.A. icing tunnel or in the Canadian N.R.C. icing tunnel is an indication that the spray water systems used in these facilities are not producing 100 per cent *subcooled* liquid droplets and may be hampered by the presence of partial "freeze-out" prior to impingement. That this does not seem to occur in the Mt. Washington tunnel may be the fortuitous result of the necessarily short distance, and, hence, time span, between the spray nozzles and the test section.

In conclusion, it is the opinion of the author that the experimental data presented in this appendix are strong evidence that the basic equations of the foregoing paper are valid. The extent of the agreement shown in the table between measured and predicted temperatures cannot be mere coincidence, since the conditions of the tests covered a wide range of icing conditions.